

Orientation dynamics of weakly Brownian particles in periodic viscous flows

Piero Olla

ISAC-CNR, Sez. Lecce, I-73100 Lecce, Italy.

Abstract

Evolution equations for the orientation distribution of axisymmetric particles in periodic flows are derived in the regime of small but non-zero Brownian rotations. The equations are based on a multiple time scale approach that allows fast computation of the relaxation processes leading to statistical equilibrium. The approach has been applied to the calculation of the effective viscosity of a thin disk suspension in gravity waves.

PACS numbers:

I. Introduction

The rheological properties of a suspension will depend, when the particles are non-spherical, on the orientation taken by the particles in response to the external flow. For a few particle shapes (e.g. the case of the ellipsoid [1]), equations for the rotation dynamics exist in closed form, and it is possible to determine the orientation distribution of the particles in suspension in the given flow. However, unless a mechanism for the achievement of a statistical equilibrium is introduced, the orientation distribution will depend on the state in which the suspension is prepared initially. In the case of microscopic particles, one such mechanism is provided by Brownian rotations [2]. It is still unclear whether inertia and interaction with other particles may contribute to the equilibration mechanism.

An equilibrium distribution could be achieved alternatively by the presence of chaos in the rotation dynamics; unfortunately, the importance of chaos turns out to be small in most situations. In the case of a simple shear and axisymmetric particles, the particle motion is periodic. This motion becomes aperiodic in the case of a time-dependent flow, but remains non-chaotic for axisymmetric particles [3]. Chaos arises in the motion of a triaxial ellipsoids in a simple shear [4], but, depending on the axis ratios, large domains of initial conditions remain associated with regular orbits and to the absence of a uniquely defined equilibrium distribution. Furthermore, for weak Brownian motion, the regular regions will act as attractors for the chaotic orbits and will provide the bulk of the orientation distribution.

The equilibrium orientation distribution of a Brownian particle has been determined in various important limit regimes. The case of strong Brownian rotation was considered by Burgers [5] leading to an orientation distribution that in first approximation can be considered isotropic. More interesting is the case of weak Brownian motion, in which the form of the equilibrium distribution is determined by the structure of the orbits in orientation space, which in turn depends on the imposed flow.

A technique for the determination of the equilibrium distribution of weakly Brownian particles, based on singular perturbation analysis of the diffusion equation in orientation space, was derived in [6] for the case of axisymmetric particles in a simple shear. In the present paper, an alternative approach will be presented, based on the perturbative determination of the orbits in orientation space. This approach which will appear to be

appropriate in the case the flow is time-dependent and, more in general, when analytical expressions for the unperturbed orbits are not available. For the sake of definiteness, the dynamics of a small disk in the field of a gravity wave will be considered, a problem with application in polar seas, where wave propagation is affected by the presence of ice crystals in suspension (frazil ice) [7, 8].

II. Unperturbed dynamics

Indicating by k and ω the wavevector and the frequency of the wave, and with h the water depth, the velocity field of a small amplitude gravity wave will have the form:

$$\begin{aligned} U_1 &= \tilde{U}[e^{-kx_2} + \alpha e^{kx_2}] \sin(kx_1 - \omega t) \\ U_2 &= \tilde{U}[e^{-kx_2} - \alpha e^{kx_2}] \cos(kx_1 - \omega t) \end{aligned} \quad (1)$$

where $\alpha = \exp(-2kh)$ and $x_2 = 0$ and $x_2 = h$ correspond respectively to the water surface and to the bottom of the basin. Due to the potential nature of the flow, the particle in suspension will see a time-dependent (periodic) pure strain field. It is convenient to carry on the calculations in the reference frame rotating with frequency $\omega/2$ around the x_3 -axis. For small amplitude waves, the particle motion is confined to a region of width $\tilde{U}/\omega \ll k^{-1}$ and kx_2 can be approximated as constant. A particle initially near the water surface at $x_1 = 0$ will thus experience the strain field $\mathbf{E} = \nabla\mathbf{U} + (\nabla\mathbf{U})^T$, with components in the rotating frame, from Eq. (1):

$$\mathbf{E} = k\tilde{U} \begin{pmatrix} 1 + \alpha \cos 2\omega t, & -\alpha \sin 2\omega t \\ -\alpha \sin 2\omega t, & -1 - \alpha \cos 2\omega t \end{pmatrix} \quad (2)$$

Thus, for deep gravity waves $\alpha = 0$ and \mathbf{E} would be a constant strain field rotating around the x_3 -axis with frequency $\omega/2$. In this reference frame, an additional vorticity field is produced:

$$\mathbf{\Omega} = \frac{\omega}{2} \begin{pmatrix} 0 & 1 \\ -1 & 0 \end{pmatrix} \quad (3)$$

This is a kind of time-dependent planar flow, of the kind described in [3], which is known to produce aperiodic behaviors in the particle orientation dynamics.

The motion of a revolution ellipsoid, with symmetry axis identified by the versor \mathbf{p} , in the presence of the strain and vorticity fields \mathbf{E} and $\mathbf{\Omega}$, is described by the Jeffery's equations [1]:

$$\dot{\mathbf{p}} = \mathbf{\Omega} \cdot \mathbf{p} + G[\mathbf{E} \cdot \mathbf{p} - (\mathbf{p} \cdot \mathbf{E} \cdot \mathbf{p})\mathbf{p}] + O((kb)^2) \quad (4)$$

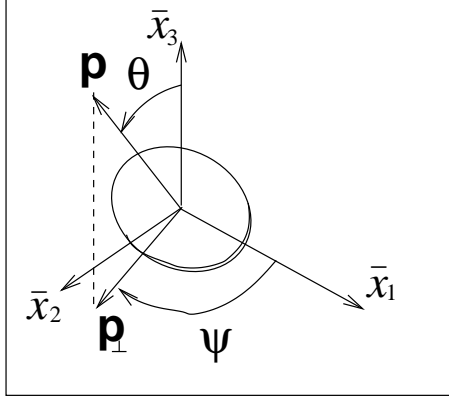


Figure 1: The coordinate system. The axes \bar{x}_i are in the rotating reference frame.

The parameter G gives the ellipsoid eccentricity, defined in terms of the particle aspect ratio $r = a/b$, where a and b are respectively along and perpendicular to the symmetry axis, by means of the relation

$$G = \frac{r^2 - 1}{r^2 + 1}$$

Introducing polar coordinates (see Fig. 1), and normalizing time and vorticity with the strain strength $e = k\tilde{U}$: $\omega \rightarrow -\omega/2Ge$ and $t \rightarrow -Get$, Jeffery's Eq. (4), using Eqs. (3) and (4), will take the form:

$$\begin{cases} \dot{\psi} = -\omega + \beta(\psi, t) \\ \dot{c} = -\frac{1}{2}\beta'(\psi, t)c \end{cases} \quad (5)$$

with dot indicating time derivative, $c = \tan \theta$ and

$$\begin{cases} \beta(\psi, t) = -\cos 2\omega t - \alpha \cos(4\omega t + 2\psi), \\ \beta'(\psi, t) \equiv \partial_\psi \beta(\psi, t) = 2[\sin 2\omega t + \alpha \sin(4\omega t + 2\psi)] \end{cases} \quad (6)$$

Following [3], the orbits can be classified studying the Poincare map $P_n(\bar{\psi}) = \text{mod}(\psi(nT|\bar{\psi}), \pi)$, with $T = \frac{\pi}{2\omega}$ the period of β , where $\psi(t|\bar{\psi})$ obeys the first of Eq. (5) with $\psi(0|\bar{\psi}) = \bar{\psi}$. It is possible to see from the first of Eq. (5) and (6) that the following relation holds:

$$P_{-n}(-\bar{\psi}) = -P_n(\bar{\psi}) \quad (7)$$

and therefore the Poincare map is symmetric under the double reflection $\{\psi, P_n\} \rightarrow \{\pi - \psi, \pi - P_n\}$ (see Fig. 2).

A periodic ψ will be associated with a fixed point in the Poincare map and will correspond to coherent orientation of the particles. As it is clear in the case of deep gravity

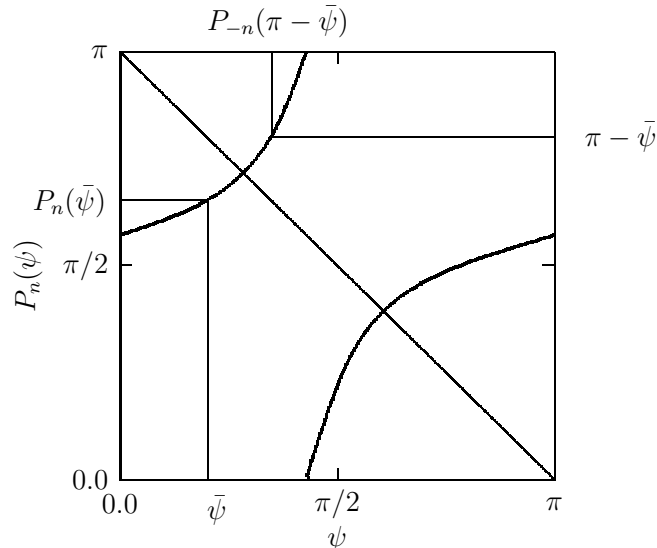


Figure 2: Symmetry of the Poincaré map for the dynamics of Eqs. (5,6). Values of the parameters: $\omega = 1.4$, $kh = 0.5$, $n = 1$; $G < 0$ (oblate ellipsoid). From Eq. (7), one has that $P_{-n}(\pi - \psi) = \pi - P_n(\psi)$ and therefore the plot is symmetric under reflection across the diagonal line $P_n = \pi - \psi$.

waves [9], this regime is produced by the aligning effect of strain on the particle dynamics. It was noted in [3] that a stable fixed point for ψ implies a value of $\beta' < 0$ negative on the average along the orbit, and, from the second of Eq. (5), an associated fixed point $\theta = \pi/2$. As can be seen in Fig 3a, this fixed point is located at $\psi > \pi/2$. The equilibrium orientation distribution will be given by the fixed points of $P_n(\bar{\psi})$, with the effect of Brownian rotations disappearing in the zero noise limit.

The alternative regime, corresponding to random particle orientation, is associated with $|\psi(nT)|$ increasing monotonously with n , with $P_n(\psi)$ generally aperiodic. In this case, from continuity of $\psi(t|\bar{\psi})$, $P_n(\bar{\psi})$ will be topologically equivalent to an irrational rotation, and the sequence $P_n(\bar{\psi})$ originating from a single $\bar{\psi}$ will fill densely the interval $[0, \pi]$. An ergodic property is then satisfied, i.e. it is possible to calculate averages over ψ as time averages. Furthermore, from Poincaré recurrence, the $P_n(\bar{\psi})$ sequence will come arbitrarily close to the initial condition for some n . Hence statistical averages can be approximated by time averages over a periodic orbit. Notice also that, from the symmetry of $P_n(\bar{\psi})$ described in Eq. (7) and Figs. 2 and 3b, if, for certain n and $\bar{\psi}_0 < \pi/2$ $|P_n(\bar{\psi}_0) - \bar{\psi}_0| \simeq 0$,

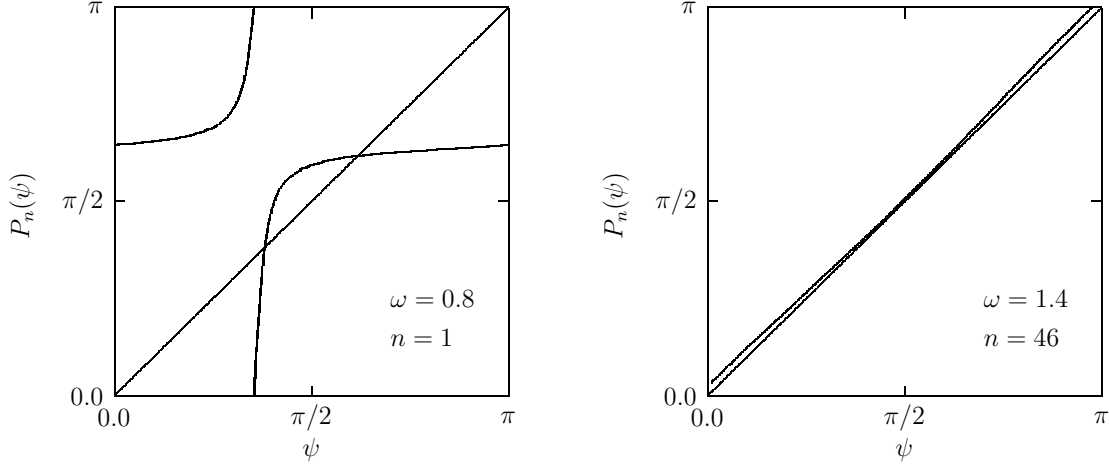


Figure 3: Poincaré map for the coherent orientation (a) and the random orientation regime (b) of an oblate ellipsoid in a shallow water wave with $kh = 0.5$. Notice in case (a) the stable fixed point at $\psi > \pi/2$ and the unstable one at $\psi < \pi/2$. With prolate ellipsoids, the fixed points would have been exchanged. The value of n in the random orientation case has been chosen to lead to approximately closed orbits. Notice that $\psi = \pi/2$ remains the best approximation to a fixed point (i.e. a closed orbit of period nT).

then, for the same n , $|P_n(\bar{\psi}) - \bar{\psi}| \simeq 0 \forall \bar{\psi} \in [\bar{\psi}_0, \pi - \bar{\psi}_0]$.

Turning to the polar angle, if the orbit in ψ approximately closes, also $c(nT|\bar{c}, \bar{\psi})$ will come arbitrarily close to the initial condition $c(0|\bar{c}, \bar{\psi}) = \bar{c}$. Hence, to identify orbits that are almost closed, it is sufficient to look for recurrence of the Poincaré map $P_n(\bar{\psi})$. To see why this property holds, notice that

$$c(nT|\bar{c}, \bar{\psi}) = \bar{c} \exp \left\{ -\frac{1}{2} \int_0^{nT} \beta'(\psi(t|\bar{\psi}), t) dt \right\}$$

which will coincide with \bar{c} when the difference

$$\psi(nT|\bar{\psi}) - \bar{\psi} = -n\omega T + \int_0^{nT} \beta(\psi(t|\bar{\psi}), t) dt$$

is constant with respect to $\bar{\psi}$, i.e. $\partial_{\bar{\psi}}[\psi(nT|\bar{\psi}) - \bar{\psi}] \simeq 0$. But, if $P_n(\bar{\psi}_0) - \bar{\psi}_0 \simeq 0$ for some $\bar{\psi}_0 < \pi/2$, we have seen that $|P_n(\bar{\psi}) - \bar{\psi}| \simeq 0 \forall \bar{\psi} \in [\bar{\psi}_0, \pi - \bar{\psi}_0]$ and $\psi(nT|\bar{\psi}) - \bar{\psi}$ is approximately constant in the interval. Hence $|c(nT|\bar{c}, \bar{\psi}) - \bar{c}| \simeq 0$ as requested.

III. The effect of noise

The fact that the orbits close when, for appropriate values of n $P_n(\bar{\psi}) \simeq \bar{\psi}$, has the consequence that these orbits can be labelled by the value $c(nT|\bar{c}, \bar{\psi}) \simeq \bar{c}$ taken by $\tan \theta$ at their starting point. As in the time independent case described in [6], the particle orientation distribution will receive a contribution from the motion along a single Jeffery trajectory and one from the distribution of the trajectories, i.e. the distribution of c at the recurrent points $t_i = n_i T$ $i = 1, 2, \dots$ where $c(t_i|\bar{c}, \bar{\psi}) \simeq \bar{c}$. If Brownian rotations were strictly zero, the PDF (probability distribution function) $\rho(c, t)$ would be itself recurrent at the times t_i : $\rho(c, t_i) = \rho(c, 0)$ and no equilibrium PDF would exist.

In the case of weak Brownian motion, an equilibrium distribution for \bar{c} exists and is obtained studying the noise produced deviation of $c(t|\bar{c}, \bar{\psi})$ away from \bar{c} at the times $t_i = n_i T$, at which the unperturbed Jeffery's orbits would approximately close.

Accounting for the effect of Brownian rotations, the Jeffery's equations will read (see Appendix A):

$$\begin{cases} d\psi = [-\omega + \beta(\psi, t)]dt + D^{1/2}g^{1/2}(c)dW_\psi \\ dc = [-\frac{1}{2}\beta'(\psi, t) + Df(c)]dt + D^{1/2}h^{1/2}(c)dW_c \end{cases} \quad (8)$$

where D has the meaning of a diffusion constant, dW_k , with $k = \psi, c$, are the Brownian increments [10]:

$$\langle dW_k \rangle = 0, \quad \langle dW_k dW_j \rangle = \delta_{kj} dt \quad (9)$$

and the functions f , g and h are given by:

$$f(c) = \frac{1}{c}(1+c^2)\left(\frac{1}{2}+c^2\right), \quad g(c) = \frac{1}{c^2}+1, \quad \text{and} \quad h(c) = (1+c^2)^2 \quad (10)$$

The deviation of $c(t|\bar{c}, \bar{\psi})$ away from \bar{c} will then be determined by the correction $\{\psi(nT|\bar{\psi}) - \psi_0(nT|\bar{\psi}), c(nT|\bar{c}, \bar{\psi}) - c_0(nT|\bar{c}, \bar{\psi})\}$, where $\{\psi_0, c_0\}$ is the unperturbed orbit obeying Eq. (5):

$$\begin{cases} \dot{\psi}_0 = -\omega + \beta_0 \\ \dot{c}_0 = -\frac{1}{2}\beta'_0 c_0 \end{cases} \quad (11)$$

with $\beta_0 = \beta(\psi_0, t)$ and similarly for β'_0 . For small noise, the correction can be determined as an expansions in powers of $D^{1/2}$: $\psi = \psi_0 + \psi_{1/2} + \psi_1 + \dots$ and similarly for c , with the initial condition $\psi_k(0) = c_k(0) = 0$ for $k > 0$. The lowest order correction is obtained from

linearization of Eq. (8) around $\{\psi_0, c_0\}$:

$$\begin{cases} d\psi_{1/2} = \beta'_0 \psi_{1/2} dt + D^{1/2} g_0^{\frac{1}{2}} dW_\psi \\ dc_{1/2} = [2\beta_0 c_0 \psi_{1/2} - \frac{1}{2}\beta'_0 c_{1/2}] dt + D^{\frac{1}{2}} h_0^{\frac{1}{2}} dW_c \end{cases} \quad (12)$$

From Eq. (9) and from linearity of Eq. (12) $\langle \psi_{1/2} \rangle = \langle c_{1/2} \rangle = 0$. The covariance equations obtained from Eq. (12) are:

$$\begin{cases} \frac{d}{dt} \langle \psi_{1/2}^2 \rangle = 2\beta'_0 \langle \psi_{1/2}^2 \rangle + Dg_0 \\ \frac{d}{dt} \langle \psi_{1/2} c_{1/2} \rangle = \frac{1}{2}\beta'_0 \langle \psi_{1/2} c_{1/2} \rangle + 2\beta_0 c_0 \langle \psi_{1/2}^2 \rangle \\ \frac{d}{dt} \langle c_{1/2}^2 \rangle = 4\beta_0 c_0 \langle \psi_{1/2} c_{1/2} \rangle - \beta'_0 \langle c_{1/2}^2 \rangle + Dh_0 \end{cases} \quad (13)$$

and lead to a diffusion contribution to the deviation. To obtain the drift contributions, it is necessary to consider the next order in the expansion of Eq. (8), and the result is:

$$\begin{cases} \frac{d}{dt} \langle \psi_1 \rangle = \beta'_0 \langle \psi_1 \rangle - 2\beta_0 \langle \psi_{1/2}^2 \rangle \\ \frac{d}{dt} \langle c_1 \rangle = -\frac{1}{2}\beta'_0 \langle c_1 \rangle + 2\beta_0 c_0 \langle \psi_1 \rangle + 2\beta_0 \langle \psi_{1/2} c_{1/2} \rangle + \beta'_0 c_0 \langle \psi_{1/2}^2 \rangle + Df_0 \end{cases} \quad (14)$$

The lowest order contributions to diffusion and drift are therefore both $O(D)$, as they should. Some simplifications of Eqs. (13-14) are still possible and are illustrated in Appendix A.

What needs to be done at this point is to extract from the deviation $\{\psi(nT|\bar{\psi}) - \psi_0(nT|\bar{\psi}), c(nT|\bar{c}, \bar{\psi}) - c_0(nT|\bar{c}, \bar{\psi})\}$, that part associated with percolation between Jeffery's orbits. It is then necessary to subtract the deviation component along the unperturbed orbit, which is associated with the noisy orbit not closing exactly at the recurrence time nT . The necessary operation is illustrated in Fig. 4, and it is assumed that the orbits can be parameterized locally with $\psi \equiv \psi(t|\bar{\psi})$ (this is possible if $\bar{\psi}$ is chosen away from turning points). The perturbed trajectory at $t = nT$ has reached the point $y = \{\psi(nT|\bar{\psi}), c(nT|\bar{c}, \bar{\psi})\}$, while the unperturbed one is at the same instant in $w = \{\bar{\psi}, \bar{c}\}$. It is then necessary to follow the perturbed trajectory from y to $w = \{\bar{\psi}, \bar{c} + \hat{c}\}$.

To $O(D)$, the correction \hat{c} is obtained from the equation

$$\hat{c} = c_{1/2} + c_1 - \bar{c} - (c_{1/2} - \bar{c})c_{\psi c}\psi_{1/2} \quad (15)$$

where $\bar{c} + \bar{c}$ is the coordinate on the unperturbed orbit at $\psi(nT|\bar{\psi}) \simeq \bar{\psi} + \psi_{1/2} + \psi_1$ and is given by

$$\bar{c} = c_\psi(\psi_{1/2} + \psi_1) + \frac{1}{2}c_{\psi\psi}\psi_{1/2}^2 \quad (16)$$

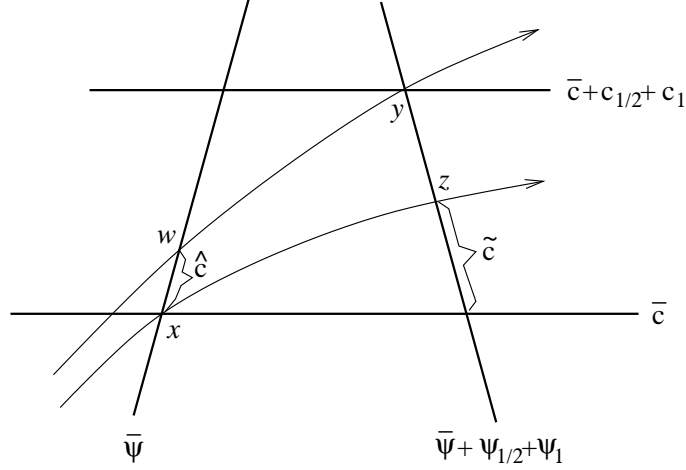


Figure 4: Orbit behavior in the proximity of the recurrent point $x = \{\bar{\psi}, \bar{c}\}$; $x - z$ unperturbed orbit; $w - y$ noisy orbit. The deviation between orbits is identified by \hat{c} .

while the piece $(c_{1/2} - \tilde{c})c_{\psi c}\psi_{1/2}$ is due to deviation between orbits passing at different c 's. Using the relation $\langle \psi_{1/2}c_{1/2} \rangle = -c_0\langle \psi_1 \rangle$ (see Appendix B), from Eqs. (15-16), the following result for the diffusion and drift across Jeffery's orbits is obtained:

$$\begin{cases} \langle \hat{c}^2 \rangle = \langle c_{1/2}^2 \rangle + c_{\psi}^2 \langle \psi_{1/2}^2 \rangle - 2c_{\psi} \langle \psi_{1/2}c_{1/2} \rangle \\ \langle \hat{c} \rangle = \langle c_1 \rangle + (c_{\psi}c_{\psi c} - \frac{1}{2}c_{\psi\psi}) \langle \psi_{1/2}^2 \rangle \end{cases} \quad (17)$$

The coefficients c_{ψ} , $c_{\psi\psi}$ and $c_{\psi c}$ entering Eqs. (15-17) give the deviation between unperturbed orbits and are given by:

$$c_{\psi} = \frac{dc_0}{d\psi}, \quad c_{\psi c} = \frac{\partial c_{\psi}}{\partial c} \quad \text{and} \quad c_{\psi\psi} = \frac{d^2c_0}{d\psi^2} \quad (18)$$

with $d/d\psi$ the derivative along the unperturbed orbit defined by

$$\frac{d}{d\psi} = \frac{1}{\dot{\psi}_0} \left[\frac{\partial}{\partial t} + \dot{\psi}_0 \frac{\partial}{\partial \psi} + \dot{c}_0 \frac{\partial}{\partial c} \right] \quad (19)$$

Combining Eqs. (18-19) with Eq. (11):

$$c_{\psi} = c_0 c_{\psi c} = \frac{\beta' c_0}{2(\omega - \beta_0)}, \quad c_{\psi\psi} = -\frac{\dot{\beta}_0 \beta_0' c_0}{(\omega - \beta_0)^3} + \frac{(\beta_0'^2 - \dot{\beta}_0') c_0}{(\omega - \beta_0)^2} - \frac{2\beta_0' c_0}{\omega - \beta_0}$$

Combining with Eqs. (11), (13) and (14), the orbit deviation (17) is therefore fully determined.

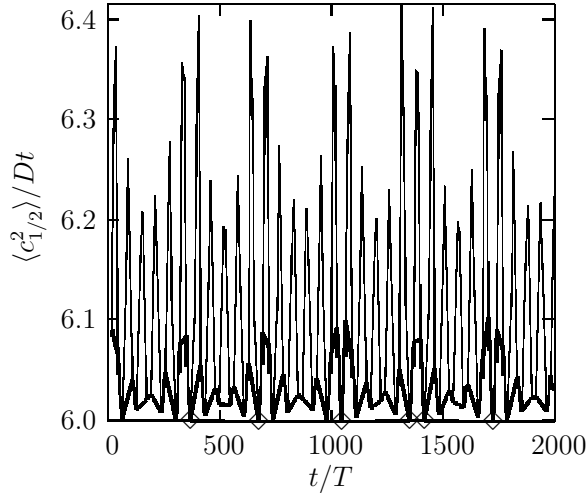


Figure 5: Determination of the diffusivity $\langle c_{1/2}^2 \rangle / Dt$ for different values of the tolerance ϵ entering the recurrence condition $|P_n(\bar{\psi}) - \bar{\psi}| < \epsilon$ with $\bar{\psi} = 0$. Values of the parameters: $\omega = 1.4$, $kh = 0.5$. Thin line $\epsilon = 0.4$; heavy line $\epsilon = 0.1$; diamonds $\epsilon = 0.01$ (the diamonds identify the actual position of the recurrence times).

IV. Determination of the orientation distribution

The quantities $\langle \hat{c}^2 \rangle$ and $\langle \hat{c} \rangle$ allow to determine the deviation of $c = \tan \theta$ from the initial condition \bar{c} , at the recurrence times $t_i = n_i T$. Both quantities are obtained from integrals along the orbits, and, for n_i large enough, it is expected that an averaging process takes place, so that the ratios $\langle \hat{c}^2 \rangle / t_i$ and $\langle \hat{c} \rangle / t_i$ tend to a limit. In Fig. 5 it is shown that this is indeed the case also for relatively large values of the tolerance ϵ , identifying recurrence through the condition $|P_n(\bar{\psi}) - \bar{\psi}| < \epsilon$. It is then possible to consider a slow time scale \bar{t} where the recurrence times t_i are treated as continuous and it is possible to introduce a Fokker-Planck equation for the PDF $\rho(\bar{c}, \bar{t})$ [10]:

$$\partial_{\bar{t}} \rho + \partial_{\bar{c}} (\bar{a} \rho) = \frac{1}{2} \partial_{\bar{c}}^2 (\bar{D} \rho) \quad (20)$$

where

$$\bar{a}(\bar{c}) = \lim_{i \rightarrow \infty} t_i^{-1} \langle \hat{c} \rangle \quad \text{and} \quad \bar{D}(\bar{c}) = \lim_{i \rightarrow \infty} t_i^{-1} \langle \hat{c}^2 \rangle \quad (21)$$

and $\langle \hat{c} \rangle$ and $\langle \hat{c}^2 \rangle$ are given in Eq. (17). Slow variation of the flow parameters entering Eq. (8) would lead to dependence of the coefficients in Eq. (20) on the slow time \bar{t} . As in

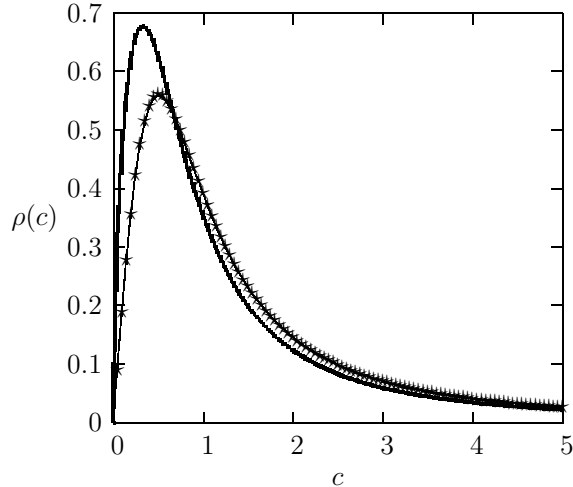


Figure 6: Comparison of the PDF $\rho(\bar{c})$ calculated using for \bar{a} and \bar{D} different values of t_i [see Eq. (21)]. Values of the parameters: $\omega = 1.4$, $kh = \infty$, $\bar{\psi} = 0$. Heavy line: $t_i = 3T$, $\epsilon = 0.4$; stars: $t_i = 20T$, $\epsilon = 0.1$; thin line: Leal & Hinch theory [6].

[6], the fact that both \bar{a} and \bar{D} depend linearly in D implies that the equilibrium PDF is independent of the noise amplitude. Statistical equilibrium will be achieved on the time scale D^{-1} . It is then necessary for the approach to be meaningful that the t_i used to define \bar{a} and \bar{D} satisfy $Dt_i \ll 1$.

Actually, excellent convergence is obtained already for t_i rather small; in the case of Fig. 6, at $t_i = 20T$, corresponding to $\epsilon = 0.1$. Notice that this is the deep water wave regime considered in [9], which, as it is clear from Eqs. (2-4), can be mapped to a constant simple shear by a redefinition of the eccentricity G ; the PDF $\rho(\bar{c})$ can then be compared with the analytical result from the theory of Leal and Hinch [6]. [In this case, the aperiodicity originates not from the dynamics, but from the sampling time T and the period of the orbit $(\omega^2 - 1)^{-\frac{1}{2}}$ being incommensurate]. As can be seen from Fig. 6, the two approaches give indistinguishable results already for $t_i = 20T$, $\epsilon = 0.1$. Similar convergence to the limit result is observed in the shallow water regime, in which comparison with the theory of Leal and Hinch is not possible.

Knowledge of the PDF $\rho(\bar{c})$ allows determination of the effective viscosity of a dilute disk suspension in the field of a wave. The viscous stress for a suspension of axisymmetric ellipsoids reads [6, 11], indicating with μ and Φ , respectively, the solvent viscosity and the

suspended phase volume fraction:

$$\boldsymbol{\sigma} = 2\mu\mathbf{E} + 2\mu\Phi\{2A\langle\mathbf{p}\mathbf{p}\mathbf{p}\mathbf{p}\rangle : \mathbf{E} + 2B[\langle\mathbf{p}\mathbf{p}\rangle \cdot \mathbf{E} + \mathbf{E} \cdot \langle\mathbf{p}\mathbf{p}\rangle] + C\mathbf{E}\} \quad (22)$$

where, in the present time dependent situation, the averages are intended over orientation and time. The coefficients $A - C$ depend on the particle geometry: [6, 9]:

$$A = \frac{5}{3\pi r} + \frac{104}{9\pi^2} - 1, \quad B = -\frac{4}{3\pi r} - \frac{64}{9\pi^2} + \frac{1}{2} \quad \text{and} \quad C = \frac{8}{3\pi r} + \frac{128}{9\pi^2}$$

with r the particle aspect ratio, supposed small. From the stress $\boldsymbol{\sigma}$, the effective viscosity $\bar{\mu}$ can be calculated in terms of the viscous dissipation in the suspension:

$$\bar{\mu} = \frac{1}{2} \frac{\boldsymbol{\sigma} : \mathbf{E}}{\mathbf{E} : \mathbf{E}} := (1 + K\Phi)\mu \quad (23)$$

where K is called the reduced viscosity. Expressing the versor \mathbf{p} in function of the angles ψ and θ , and using Eqs. (22) and (23):

$$K = A\langle\sin^4 \theta \sin^2 2\psi\rangle + 2B\langle\sin^2 \theta\rangle + C \quad (24)$$

As in [6], the average over orientation is split into parts along and transverse to the orbit. In the present situation, however, evaluation of the average along the orbit is slightly more delicate than in the time-independent case. At a generic time t the average of a function $f(\psi, c)$ will be:

$$\langle f \rangle(t) = \frac{1}{n} \sum_{i=1}^n \int d\bar{c} \rho(\bar{c}) f(\psi(t + iT|\bar{\psi}), c(t + iT|\bar{c}, \bar{\psi}))$$

Carrying on the average over a wave period, which, from Eq. (1), is equivalent also to a space average, leads to the average along an orbit:

$$\langle f \rangle = \frac{1}{nT} \int d\bar{c} \rho(\bar{c}) \int_0^{nT} dt f(\psi(t|\bar{\psi}), c(t|\bar{c}, \bar{\psi})) \quad (25)$$

Evaluating Eq. (24) with Eq. (25) leads to the values of the reduced viscosity shown in Fig. 7. The calculation has been carried on using as recurrence point $\bar{\psi} = 0$; the value of the of the particle aspect ratio has been chosen consistent with frazil ice measurements [7]. The same qualitative regime observed in the deep water case is reproduced here, namely, a dip in the reduced viscosity at the crossover from the coherent rotation regime to the

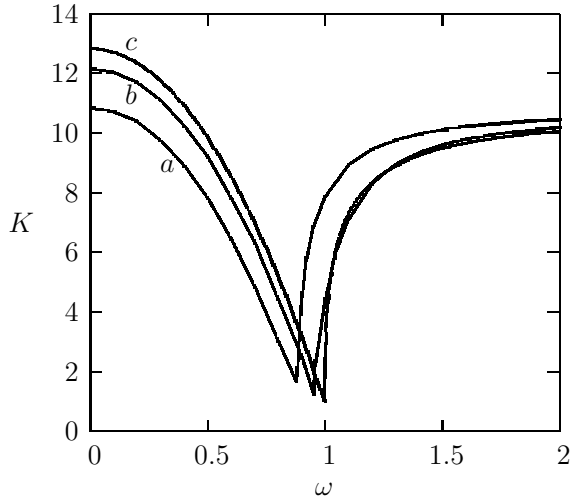


Figure 7: Reduced viscosity, averaged over a wave period, for a suspension of disk-like particles with aspect ratio $r = 0.045$. Different curves correspond to different water depths: (a) $kh = 0.25$; (b) $kh = 0.5$; (c) $kh = \infty$.

random orientation one [9]. As in the deep water case, the coherent regime is associated with high amplitude waves corresponding to small values of the normalized frequency ω . The reduced viscosity has been calculated in this range from Eq. (24), fixing $\theta = \pi/2$ and integrating the equation for ψ with initial condition at the fixed point.

V. Conclusions

The numerical evaluation of the rheological properties of a suspension of particles that are weakly Brownian is faced with difficulties associated with the long integration times necessary to achieve statistical equilibrium. Analytical techniques for the calculation of the cumulative effect of the Brownian noise on the dynamics are therefore necessary. The technique presented in this paper can be seen as a multiple time scale analysis [12] in which the stochastic dynamics is pushed to the slow scale, while the local strain and vorticity are treated as fast variables. For the periodic flows considered in this paper, the effective drift and diffusivity coefficients are obtained integrating the fast dynamics over a single periodic orbit approximating the particle orientation dynamics. Slow variations would be accounted for, sampling the approximate periodic orbits in appropriate way along the

particle trajectories, and would lead to effective drift and diffusivity coefficients depending on the slow time. Once the effective drift and diffusivity were available, a Monte Carlo, for the determination of the rheological properties of a suspension, would be carried on at the slow time scale. [In the gravity wave example of this paper, this would be associated with integration of the Fokker-Planck equation (20)],

Application of these techniques to the dynamics of a thin disk suspension in gravity waves, has shown that qualitative behaviors observed in the deep water case [9] are preserved in the shallow water regime. Precisely, a transition from a coherent rotation regime for large amplitude waves to a random orientation one, characterized by a deep minimum in the medium effective viscosity.

A natural extension of the techniques illustrated could be the treatment of higher numbers of degrees of freedom. The most immediate example is the triaxial ellipsoid in a simple shear considered in [4]. In this case, the angle θ would be replaced by the pair $\{\theta, \phi\}$ with ϕ the rotation around the axis \mathbf{p} . An analysis in the whole phase domain would require, however, consideration of the transition region from the regular orbits, in which diffusion is dominated by Brownian rotation, to the chaos dominated stochastic region. It is expected that the transition be signalled by the breakup of linear scaling in time for the drift and diffusion across orbits.

Acknowledgements

This research was carried on at the Dipartimento di Fisica dell'Università di Cagliari. The author wishes to thank Alberto Pompei for hospitality.

Appendix A. Noise term determination

The noise term to add in the Jeffery's equations (5) can be obtained directly from the diffusion equation obeyed for zero flow by the orientation PDF in the variables $\{\psi, c\}$. Alternatively, one may consider the diffusion operator in the variables $\{\psi, \theta\}$:

$$\nabla^2 = \frac{1}{\sin^2 \theta} \frac{\partial^2}{\partial \psi^2} + \frac{1}{\sin \theta} \frac{\partial}{\partial \theta} \sin \theta \frac{\partial}{\partial \theta}$$

and determine the stochastic process leading to the Fokker-Planck equation $\nabla^2 \rho(\psi, \theta) = 0$ [which has the isotropic solution $\rho(\psi, \theta) = \frac{1}{2\pi} \sin \theta$]. One finds the increments for ψ and θ

produced by Brownian rotation in the time interval dt [10]:

$$d\psi = |\sin \theta|^{-1} dW_\psi, \quad d\theta = \frac{1}{2} \cot \theta dt + dW_\theta$$

where dW_k , $k = \psi, \theta$ are the Brownian increments

$$\langle dW_k \rangle = 0, \quad \langle dW_j dW_k \rangle = \delta_{jk} dt$$

Changing then variables from θ to c and using Itô's lemma, one finds:

$$dc = d\theta \frac{dc}{d\theta} + \frac{1}{2} \langle dW_\theta^2 \rangle \frac{d^2c}{d\theta^2} = \frac{1}{c} (1 + c^2) \left(\frac{1}{2} + c^2 \right) dt + (1 + c^2) dW_\theta$$

and expressing also $\sin \theta = c(1 + c^2)^{-1/2}$ in $d\psi$, Eq. (8) is finally obtained.

Appendix B. Alternative form of the perturbed orbit equations

Equations (13-14) can be simplified, and the singularity in $\theta = 0$ produced by the noise term in the first of Eq. (8) eliminated, by the change of variables:

$$y_1 = c_0^2 \langle \psi_{1/2}^2 \rangle, \quad y_2 = c_0 \langle \psi_{1/2} c_{1/2} \rangle, \quad y_3 = \langle c_{1/2}^2 \rangle, \quad y_4 = c_0 \langle c_1 \rangle, \quad y_5 = c_0^2 \langle \psi_1 \rangle$$

In the new variables, Eqs. (13-14) take the form:

$$\begin{cases} \dot{y}_1 = \beta'_0 y_1 + D\tilde{g} \\ \dot{y}_2 = 2\beta_0 y_1 \\ \dot{y}_3 = 4\beta_0 y_2 - \beta'_0 y_3 + D\tilde{h} \\ \dot{y}_4 = -\beta'_0 y_4 + 2\beta_0 y_2 + \beta'_0 y_1 + 2\beta_0 y_5 + D\tilde{f} \\ \dot{y}_5 = -2\beta_0 y_1 \end{cases} \quad (B1)$$

where, from Eq. (10), $\tilde{g} = 1 + c_0^2$, $\tilde{h} = (1 + c_0^2)^2$ and $\tilde{f} = (1 + c_0^2) \left(\frac{1}{2} + c_0^2 \right)$. Comparing the equations for y_2 and y_5 , one sees that, thanks to the initial condition $y_k(0) = 0$, $y_2 = -y_5$ and then $\langle \psi_{1/2} c_{1/2} \rangle = -c_0 \langle \psi_1 \rangle$; thus the equation for $\langle \psi_1 \rangle$ can be eliminated from (14). Equation (B1) can then be further simplified to:

$$\begin{cases} \dot{y}_1 = \beta'_0 y_1 + D\tilde{g} \\ \dot{y}_2 = 2\beta_0 y_1 \\ \dot{y}_3 = 4\beta_0 y_2 - \beta'_0 y_3 + D\tilde{h} \\ \dot{y}_4 = -\beta'_0 y_4 + \beta'_0 y_3 + D\tilde{f} \end{cases} \quad (B2)$$

References

- [1] G.B. Jeffery, "The motion of ellipsoidal particles immersed in a viscous fluid," Proc. Roy. Soc. A **102**, 161 (1922)
- [2] G.I. Taylor, "The motion of ellipsoidal particles in a viscous fluid," Proc. Roy. Soc. A **103**, 58 (1923)
- [3] A.J. Szeri, W.J. Milliken and L.G. Leal, "Rigid particles suspended in time-dependent flows: irregular versus regular motion, disorder versus order," J. Fluid Mech. **237**, 33 (1992)
- [4] A.L. Yarin, O. Gottlieb and I.V. Roisman, "Chaotic rotation of triaxial ellipsoids in simple shear flows," J. Fluid Mech. **340**, 83 (1997)
- [5] J.M. Burgers, *Second Report on Viscosity and Plasticity* (North-Holland, Amsterdam, 1938) Chap. 3
- [6] L.G. Leal and E.J. Hinch, "The effect of weak Brownian rotations on particles in shear flows," J. Fluid. Mech. **46**, 685 (1972)
- [7] S. Martin and P. Kauffman, "A field and laboratory study of wave damping by grease ice," J. Glaciology **96**, 283 (1981)
- [8] K. Newyear and S. Martin, "A comparison of theory and laboratory measurements of wave propagation and attenuation in grease ice," J. Geophys. Res. **102**, 25091 (1997)
- [9] G. DeCarolis, P. Olla and L. Pignagnoli, "Effective viscosity of grease ice in linearized gravity waves," J. Fluid Mech. **535**, 369 (2005)
- [10] C.W. Gardiner, *Handbook for stochastic methods*, third edition (Springer NY, 2004)
- [11] E.J. Hinch and L.G. Leal, "Constitutive equations in suspension mechanics. Part 2. Approximate forms of a suspension of rigid particles affected by Brownian rotations," J. Fluid Mech. **76**, 187 (1975)
- [12] C.M. Bender and S.A. Orszag, *Advanced mathematical methods for scientists and engineers* (McGraw-Hill, NY, 1978)